I&EC research
Industrial & Engineering Chemistry Research

Article

pubs.acs.org/IECR

Reservoir Oil Characterization for Compositional Simulation of Solvent Injection Processes

Ashutosh Kumar and Ryosuke Okuno*

School of Petroleum Engineering, University of Alberta, 3-114 Markin/CNRL Natural Resources Engineering Facility, Edmonton, Alberta T6G 2W2, Canada

Supporting Information

ABSTRACT: Reliable design of solvent injection for oil recovery requires accurate representation of multiphase behavior in a wide range of pressure−temperature−composition conditions. Volume shift is often required to improve density predictions, separately from compositional behavior predictions, in conventional fluid characterization methods (CM). Thermodynamically, however, volumetric behavior predictions are consequences of compositional behavior predictions. We develop a new fluid characterization method (NM) that gives accurate multiphase behavior representation for oil/solvent mixtures without volume shift. The Peng−Robinson EOS is used with the van der Waals mixing rules. The NM is compared with the CM in terms of phase diagrams, minimum miscibility pressure calculations, and oil displacement simulations. It is shown that the CM with volume shift can give erroneous phase behavior and oil recovery predictions. The NM requires no volume shift to achieve accurate predictions of compositional and volumetric phase behaviors. The two types of phase behaviors are properly coupled in the NM.

1. INTRODUCTION

Solvent methods for enhanced oil recovery and heavy-oil recovery have been studied and implemented in oil fields (e.g., Mohanty et al.;[1] DeRuiter et al.[2]). Various steam/solvent coinjection schemes are also proposed in the literature[3−7] to improve efficiency of the conventional steam-assisted gravity drainage. Reliable design of such oil recovery processes requires compositional reservoir simulation to model mass transfer among phases using a cubic equation of state (EOS).

Cubic EOSs are widely used in the petroleum industry to model volumetric and compositional phase behavior of conventional oils. The most widely used cubic EOSs are the Peng−Robinson (PR) EOS[8,9] and the Soave−Redlich−Kwong (SRK) EOS.[10] These EOSs together with the van der Waals mixing rules are suitable for computationally efficient representation of vapor−liquid equilibrium for hydrocarbon mixtures at a wide range of pressures (Okuno et al.[11]).

However, application of these EOSs for modeling heavy-oil recovery is not straightforward. For heavy-oil recovery, a typical operation range in pressure−temperature−composition (*P-T-x*) space is much wider than that for enhanced recovery of conventional oil. When steam and solvent are coinjected for heavy-oil recovery, reservoir temperatures lie between an initial reservoir temperature and steam temperatures (e.g., between 290 and 530 K for a typical solvent-steam-assisted gravity drainage). Also, mixtures of solvent and heavy oils are highly size-asymmetric, resulting in a wider variety of composition conditions. The wide operation range in *P-T-x* space provides technical challenges for the traditional use of cubic EOSs with the van der Waals mixing rules.

Fluid characterization using an EOS is conducted based on experimental data available, which typically consist of composition analysis and pressure−volume−temperature (PVT) data. However, it can be difficult to take reliable downhole fluid samples for heavy oil (Memon et al.;[12] Zabel et al.[13]). Even when a reliable sample is available for a heavy oil, its detailed composition is uncertain because of high concentrations of nonidentifiable compounds. Availability of experimental data in *P-T-x* space, especially at different composition conditions, is often limited for heavy oil mainly because of its high viscosity and highly uncertain composition. Laboratory measurements are performed at certain *P-T-x* conditions. It is difficult to measure phase behavior along the compositional path for a given solvent injection in the laboratory. Use of a reliable fluid characterization method is as important as use of reliable experimental data to predict phase behavior during solvent injection processes in compositional simulation. Heavy-oil PVT data that are measurable include saturation pressures (P_{SAT}) and densities at different conditions. It is not unusual that they are the only reliable PVT data for a heavy oil.

Characterization of conventional oils using an EOS has been developed and implemented in commercial software.[14,15] A typical characterization process consists of four main steps as follows:

Step 1. Estimation of a molar distribution with respect to molecular weight (MW) or carbon number (CN) to split the plus fraction (e.g., C_{7+}) into detailed components.

Step 2. Estimation of properties for the detailed components such as critical temperature (T_C), critical pressure (P_C), critical volume (V_C), acentric factor (ω), and volume shift parameters.

Received: July 10, 2013
Revised: December 1, 2013
Accepted: December 13, 2013
Published: December 13, 2013

   dx.doi.org/10.1021/ie402198z | *Ind. Eng. Chem. Res.* 2014, 53, 440−455

Step 3. Grouping of the detailed components into fewer pseudocomponents.

Step 4. Regression of pseudocomponents' properties to match experimental data available.

In step 1, a distribution function is fitted to the composition analysis data available. Forms of distribution functions proposed in the literature include the gamma,[16] chi-squared,[17] and logarithmic distributions.[18,19] The gamma distribution is the most general form among the three and reduces to the other two when certain assumptions are used. The logarithmic distribution is a widely used form for conventional oil characterization, where composition analysis can provide composition information for a large fraction of the fluid. Heavy oils often require more flexible distribution functions, such as the gamma and chi-squared ones, to match their composition analysis data (Ghasemi et al.[20]). Regardless of the type of the distribution function used, however, the reliability of the resulting molar distribution depends primarily on how much uncertainty is left as a plus fraction in composition analysis.

Step 2 uses correlations to estimate properties of the split components because critical properties measured for hydrocarbons heavier than C_{24} are not available (Ambrose and Tsonopoulos[21]). These correlations include Cavett,[22] Edmister,[23] Kesler and Lee,[24] Riazi and Al-Sahaff,[25] Korsten,[26] Riazi and Daubert,[27,28] Twu,[29] and Lee and Kesler.[30] The correlations of Pedersen et al.[31−33] are functions of MW and density at atmospheric conditions, which are in turn functions of CN. These correlations are developed for an EOS to reproduce vapor pressures and the critical point for the pseudocomponent of a given CN. However, the PR and SRK EOSs with these correlations cannot accurately model densities of heavy hydrocarbons unless volume shift parameters[34,35] are used. Krejbjerg and Pedersen[36] developed new correlations for T_C, P_C, and ω for heavy-oil characterization. Their correlations do not attempt to model three-hydrocarbon-phase behavior, although such phase behavior often occurs for highly asymmetric mixtures of heavy oil with solvent (Polishuk et al.[37]).

Step 3 reduces the number of components used in the fluid model and calculates properties of each pseudocomponent by averaging over its member components. Use of fewer components can make EOS calculations more efficient, but it can also result in erroneous predictions of phase behavior due to reduced dimensionality in composition space. Common grouping procedures in the literature include the ones of Pedersen et al.[19] and Whitson and Brulè.[14] The former uses the equal mass grouping with mass-weighted averaging of properties, while the latter uses the Gaussian quadrature grouping method with mole-weighted averaging.

In the equal mass grouping approach, detailed split components are grouped into fewer pseudocomponents that have an approximately same mass. The critical properties for a pseudocomponent are estimated by taking the mass-weighted average of the critical properties of member components for that pseudocomponent. In the Gaussian quadrature grouping method of Whitson and Brulè,[14] each pseudocomponent has a wider range of molecular weights, and a component may be present in multiple pseudocomponents (Pedersen and Christensen[15]). Representative critical properties for a pseudocomponent are estimated by taking the mole-weighted average of critical properties of member components for that pseudocomponent. Joergensen and Stenby[38] conducted a comparative study of 12 different grouping methods and concluded that it was difficult to single out the best grouping method.

As mentioned before, simulation of solvent methods for heavy-oil recovery requires reliable representation of phase behavior at a wide range of composition conditions. Therefore, a reliable fluid model for solvent/heavy-oil mixtures often requires more components than that for solvent/conventional-oil mixtures.

Step 4 is often needed because each of steps 1−3 makes certain assumptions resulting in deviations of predictions from actual phase behavior. Regression procedures for conventional oil characterization are discussed in detail in Whitson and Brulè[14] and Pedersen and Christensen.[15] Typical parameters adjusted in this step include T_C, P_C, ω, volume shift parameters, and binary interaction parameters (BIPs) for pseudocomponents. The constant terms of the attraction and covolume parameters of a cubic EOS, Ω_a and Ω_b, are sometimes adjusted, but this is not recommended, as explained by Wang and Pope.[39] These adjustment parameters offer flexibility that may be required to match various types of PVT data such as P_{SAT}, constant mass expansion, constant volume depletion, differential liberation, separator tests, swelling tests, minimum miscibility pressures, and viscosity data. Different EOS fluid models can result depending on which parameters are adjusted and how much they are adjusted (Lolley and Richardson[40]).

As described above, each of steps 1−4 is more difficult for heavy oil than for conventional oil. The main reason for the difficulties is that heavy-oil characterization is conducted under high uncertainties in oil composition, components' properties (e.g., T_C, P_C, and ω), and phase behavior in *P-T-x* space. Also, considering direct use of EOS fluid models in compositional simulation, it is undesirable that modeling heavy-oil/solvent mixtures often requires many components to accurately model their phase behavior.

In this research, a new characterization method is developed for simulation of enhanced oil recovery and heavy-oil recovery. The uncertainty issues discussed above are addressed by incorporating physical observations into our procedures for critical parameter estimation, step 2, and regression, step 4. Since density data are easier to obtain than composition data, our method effectively uses density data to improve phase behavior predictions in *P-T-x* space; that is, volume shift parameters are not required in our characterization method. In the following section, the conventional characterization method used in this research is defined. We then present a new characterization method and its application to 22 different reservoir oils. Comparisons are made between the new and conventional characterization methods in terms of phase behavior predictions in *P-T-x* space for actual reservoir oils and their mixtures with solvents.

2. CONVENTIONAL CHARACTERIZATION METHOD USED IN THIS RESEARCH

The conventional characterization method used in this research is based mainly on Pedersen and Christensen[15] and Wang and Pope.[39] The method of Pedersen and Christensen[15] has been implemented in the PVTsim software of Calsep.[41] Descriptions are given below for the conventional characterization steps 1−4 (see the introduction section for the definitions of the steps). All characterizations in this research assume that PVT data available include the oil composition, the oil P_{SAT} at the

dx.doi.org/10.1021/ie402198z | Ind. Eng. Chem. Res. 2014, 53, 440−455

reservoir temperature, and liquid densities and viscosities at different pressures at the reservoir temperature. All EOS calculations in this research use the PR EOS, eq 1, with the van der Waals mixing rules.

$$p = \frac{RT}{v - b} - \frac{a_c\alpha(T)}{v^2 + 2bv - b^2} \quad (1)$$

where

$$a_c = 0.457235529\frac{(RT_c)^2}{P_c}$$

$$b = 0.077796074\frac{RT_c}{P_c}$$

$$\sqrt{\alpha(T)} = \left[1 + m\left(1 - \left(\frac{T}{T_c}\right)^{0.5}\right)\right]$$

$$m = 0.37464 + 1.54226\omega - 0.26992\omega^2 \quad \text{for} \quad \omega < 0.49 \quad (2)$$

$$m = 0.379642 + 1.48503\omega - 0.164423\omega^2 + 0.016666\omega^3 \quad \text{for} \quad \omega \geq 0.49 \quad (3)$$

Step 1 of the conventional method assumes a logarithmic distribution for splitting a plus fraction. In step 2, critical properties, such as T_C, P_C, and ω, are estimated using Krejbjerg and Pedersen.[36] Step 3 uses the equal-mass grouping with mass-weighted averaging of properties.

Although there is no well-defined regression scheme for step 4 due to its high flexibility in the conventional method, Figure S1 in the Supporting Information depicts the conventional regression scheme used in this research, which is based on Pedersen and Christensen[15] and Christensen.[42] Adjustments are made for T_C, P_C, and ω of pseudocomponents to match the P_{SAT} at the reservoir temperature. Adjustment parameters are selected based on their sensitivities to P_{SAT} calculation (Voulgaris et al.[43]).

After matching the P_{SAT}, density data at different pressures at the reservoir temperature are matched. We consider two options here; one is to adjust T_C, P_C, and ω, and the other to adjust volume-shift parameters (the C_{PEN} parameters in the PVTsim software). The second option is widely used in the literature. In this paper, the conventional methods with the first option and with the second option are referred to as the $CM_{w/o}V$ and CM_wV, respectively. The $CM_{w/o}V$ and CM_wV are collectively called the CM. The CM_wV will be compared with our new method (NM) developed in the next section, both with 11 components. The $CM_{w/o}V$ will be used with 30 components to generate pseudodata for the comparisons. The regression step confirms that T_C and P_C have physically correct trends with respect to MW; that is, T_C monotonically increases and P_C monotonically decreases with increasing MW.

V_C for pseudocomponents are also adjusted to match viscosity data using the Lohrenz−Bray−Clark (LBC) model.[44] BIPs are not adjusted in this research. These two notes also apply for the NM described in the next section.

The PVTsim software is used as part of the CM because its flexibility enables to apply the most prevalent characterization procedure in the literature (see Figure S1 in the Supporting Information). It requires stepwise manual adjustment of parameters based on engineering judgments, which can be done with PVTsim. In the CM, T_C, P_C, and ω for each pseudocomponent are tuning parameters. For example, use of four pseudocomponents results in 12 adjustment parameters. Parameter values resulting from a regression process depend on the weights assigned to sets of experimental data, the ranges of variation allowed for parameters, and the order of parameter adjustments. Special care must be taken by experienced engineers to ensure smooth and physically justifiable curves for T_C, P_C, and ω with respect to MW. Automated robust characterization is possible when the automatic regression keeps physically justifiable trends of parameters, which is achieved in the NM as will be discussed. Note that the NM also satisfies Pitzer[45] and Pitzer et al.'s[46] definition of acentric factor for each component.

3. NEW CHARACTERIZATION METHOD BASED ON PERTURBATION FROM N-ALKANES

The new characterization method (NM) developed in this section addresses two major issues that the CM can pose when applied for heavy-oil characterization. These issues, which are described below, come essentially from the fact that heavy-oil characterization must be conducted under high uncertainties in oil composition, components' properties (e.g., T_C, P_C, and ω), and phase behavior in P-T-x space. In the following subsections, we first describe the issues of the CM. Our development of the NM is then presented in detail.

3.1. Issues of The Conventional Method. One of the two major issues is in step 2, estimation of pseudocomponents' properties. Conventional correlations for pseudocomponents' properties in the literature are typically functions of two parameters (e.g., MW and specific gravity). The fundamental reason for use of two types of parameters is that a CN group contains a wide variety of compounds. One way to categorize hydrocarbon compounds is paraffins, naphthenes, and aromatics (PNA). T_C and P_C of paraffins are in general lower than those of aromatics within a given CN group (Kumar and Okuno[47]). The trend is the other way around for ω. That is, one of the two parameters, specific gravity, is required to consider the effects of a PNA distribution within a CN group on critical properties of the CN group. However, specific gravities of pseudocomponents in a plus fraction are unknown. They are then estimated using a function of CN in Pedersen and Christensen.[15] In this way, a certain PNA distribution is implicitly assumed in the CM for property estimation, and the PNA distribution assumed is not well-defined for users.

The PNA distribution implicitly set is coupled with a shortcoming of cubic EOSs in the CM. That is, even when T_C, P_C, and ω of a well-defined hydrocarbon (e.g., a n-alkane compound) are given, cubic EOSs are inaccurate in predicting its liquid densities unless a volume shift parameter is used (Ting et al.;[48] Voutas et al.;[49] Yakoumis et al.[50]). This shortcoming of cubic EOSs is more serious for heavier hydrocarbons (Kumar and Okuno[51]). Regression in step 4 then attempts to decrease errors caused by the coupled problem mentioned above, where adjustments of T_C, P_C, and ω must be performed with little justification in a physical sense.

Another major issue addressed in this research is the separation of volumetric and compositional behaviors using volume shift parameters in the CM_wV. For heavy oil, available experimental data are mostly volumetric ones, instead of compositional ones. Volume-shift parameters are typically needed when the CM is used with a small number of components to match heavy-oil density data. In such a case,

dx.doi.org/10.1021/ie402198z | Ind. Eng. Chem. Res. 2014, 53, 440−455

compositional behavior predictions of the resulting fluid model depend significantly on how much one relies on volume shift parameters to match density data.

Thermodynamically, however, volumetric phase behavior, including densities, is a consequence of compositional phase behavior; that is, compositional and volumetric phase behaviors should not be modeled separately. Density data for a given fluid contain its composition information. The CM_wV does not effectively use density data to improve compositional phase behavior predictions. Although composition analysis is often difficult for heavy oils, density data can supplement compositional data for heavy-oil characterization by minimizing use of volume-shift parameters. Thus, our NM does not use volume-shift parameters, which can also reduce the number of adjustment parameters. Section S2 in the Supporting Information presents the effects of volume shift parameters on the Gibbs free energy when used as regression parameters in reservoir oil characterization.

3.2. Characterization Steps in the New Method. The most important novelties of the NM lie in steps 2 and 4 as will be described below. For steps 1 and 3, the NM is based on Quiñones-Cisneros et al.;[17,52−54] that is, the chi-squared distribution is used for step 1, and the equal-mass grouping with mass-weighted averaging of properties is used for step 3.

Step 2, estimation of T_C, P_C, and ω for pseudocomponents, in the NM is based on the correlations of Kumar and Okuno.[51] The PR EOS with the correlations gives accurate predictions of liquid densities and vapor pressures for *n*-alkanes from C_7 to C_{100} without using volume-shift parameters. These correlations were developed using the optimized critical parameters and *m* parameters for the PR EOS for *n*-alkanes from C_7 to C_{100}. The optimized critical values do not represent the physical critical points. In reservoir oil characterization, however, physical critical points of pseudocomponents are not well-defined at first.

Only *n*-alkane compounds can form a well-defined homologous hydrocarbon series. There are sufficient experimental data for the homologous series of *n*-alkane compounds in the literature, which were used in Kumar and Okuno.[51]

The NM considers a PNA distribution of a plus fraction as perturbation from a limiting distribution of 100% *n*-alkanes. Considering the trends of T_C, P_C, and ω with respect to the PNA distribution, T_C and P_C of a pseudocomponent should be higher than the *n*-alkane values from the correlations of Kumar and Okuno.[51] Similarly, ω of a pseudocomponent should be lower than the n-alkane values. The amounts of perturbations in T_C, P_C, and ω from the *n*-alkane values are related to the concentration of components other than *n*-alkanes, especially aromatic components, in the plus fraction. Step 2 of the NM combines the perturbation concept and the correlations of Kumar and Okuno,[51] as given in eqs 4, 5, and 6.

$$T_c = 1154.35 - 844.83(1.0 + 1.7557 \times 10^{-3} f_T \mathrm{MW})^{-2.0} \quad (4)$$

$$P_c = 559.93\left(\frac{\mathrm{MW}}{f_P}\right)^{-0.638} - 1.49 \quad (5)$$

$$m = 0.4707 + 2.4831(f_m \mathrm{MW})^{-\left(\frac{39.933}{f_m \mathrm{MW}}\right)} \quad (6)$$

The *m* parameter in eq 6 is defined in eqs 2 and 3 as a one-to-one function of ω.

The perturbation factors for T_C, P_C, and *m* are expressed as f_T, f_P, and f_m, respectively. These perturbations are qualitative deviation of pseudocomponents from *n*-alkane behavior. The perturbed values are valid only with the cubic EOS used. Equations 4−6 reduce to the correlations of Kumar and Okuno[51] for *n*-alkanes when the perturbation factors are 1.0. As a pseudocomponent deviates from the *n*-alkane with the same MW, f_T and f_P increase, and f_m decreases from the value of 1.0.

Equations 4−6 also consider another physical trend that can be derived from the correlations of Riazi and Al-Sahhaf[25] and Pan et al.[55] Using their correlations, the differences between aromatics and paraffins in terms of T_C and P_C decrease with increasing MW (Figures 1 and 2). In terms of *m*, the difference

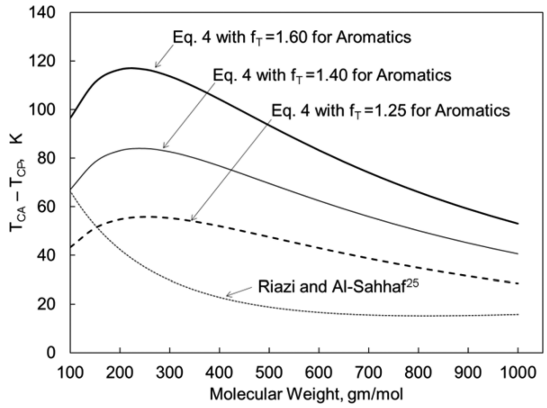

Figure 1. Differences between aromatics and paraffins for critical temperature, $T_{CA}-T_{CP}$, based on the correlations of Riazi and Al-Sahhaf[25] and eq 4. T_{CA} using eq 4 assumes three different f_T values for aromatics, 1.25, 1.40, and 1.60. T_{CP} using eq 4 uses f_T of 1.0.

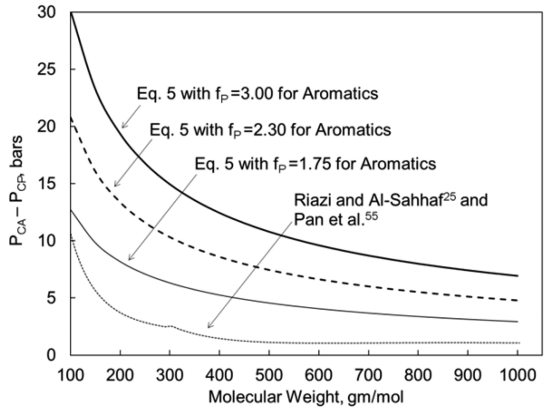

Figure 2. Differences between aromatics and paraffins for critical pressure, $P_{CA}-P_{CP}$, based on the correlations of Riazi and Al-Sahhaf,[25] Pan et al.,[55] and eq 5. P_{CA} using eq 5 assumes three different f_P values for aromatics, 1.75, 2.30, and 3.0. P_{CP} using eq 5 uses f_P of 1.0. The correlation of Pan et al.[55] is used for molecular weight larger than 300 g/mol.

exhibits a maximum around MW of 500 g/mol as shown in Figure 3. These curves indicate that the effects of nonalkane compounds on T_C, P_C, and *m* vary with MW.

Figures 1−3 also show how T_C, P_C, and *m* in our eqs 4−6 deviate from their *n*-alkane values as the perturbation factors (f_T, f_P, and f_m) change from unity. Figures 1−3 present that eqs 4−6 qualitatively represent the physical trends mentioned above. Figure 1 shows that the sensitivity of T_C to f_T in eq 4 exhibits a maximum around MW of 200 g/mol, which is not

dx.doi.org/10.1021/ie402198z | Ind. Eng. Chem. Res. 2014, 53, 440−455

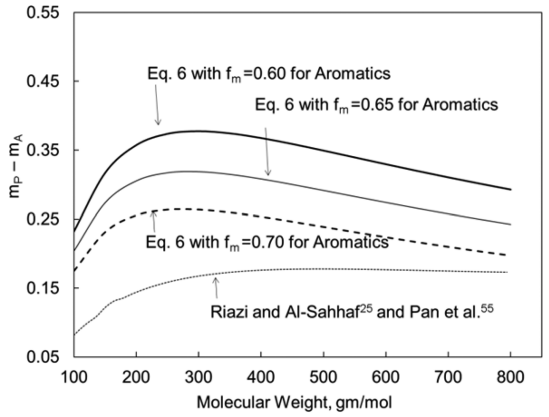

Figure 3. Differences between aromatics and paraffins for the m parameter, $m_P - m_A$, based on the correlations of Riazi and Al-Sahhaf,[25] Pan et al.,[55] and eq 6. The m parameter is defined in eqs 2 and 3. m_A using eq 6 assumes three different f_m values for aromatics, 0.60, 0.65, and 0.70. m_P using eq 6 uses f_m of 1.0. The correlation of Riazi and Al-Sahhaf[25] is used for m_P, and the correlation of Pan et al.[55] is used for m_A.

observed from the correlations of Riazi and Al-Sahhaf.[25] However, the behavior of T_C with respect to f_T in the MW range 100−200 g/mol does not affect practical fluid characterization because most of pseudocomponents are out of this MW range, especially for heavy oils.

Step 4 of the NM uses eqs 4−6 to regress T_C, P_C, and m of pseudocomponents for matching P_{SAT} and density data. Figure S2 and the summary of step 4 given in section S1 (in the Supporting Information) present the algorithm to adjust f_T, f_P, and f_m. There are three main iteration loops, the P_{SAT}, density, and ω loops. The P_{SAT} loop is the innermost loop contained by the density loop. The ω loop contains the other two loops.

The initial values for f_T and f_P are 1.0. The f_m parameter is initialized by solving eq 7:

$$0.6 = 0.4707 + 2.4831(f_m \mathrm{MW}_1)^{-\left(\frac{39.933}{f_m \mathrm{MW}_1}\right)} \tag{7}$$

where MW_1 is the MW of the lightest pseudocomponent in a fluid model. The value on the left side of eq 7 (i.e., 0.6) is lower than the m for benzene, 0.6866 (see eq 2 with ω = 0.21). Use of eq 7 assumes all pseudocomponents are heavier than C_6. The value 0.6 can be unduly low if MW_1 is much greater than the MW of benzene. However, this value is recommended for robustness.

In the P_{SAT} loop, f_P is adjusted by Δf_P (e.g., $+10^{-6}$) per iteration to match the P_{SAT} by decreasing the ψ function (eq 8). Once the ψ function becomes smaller than a tolerance (e.g., 10^{-4}), the density loop decreases the δ function (eq 9) by adjusting f_T and f_P. In the density loop, f_P is set to 1.0 at the beginning of each iteration, and f_T is adjusted by Δf_T (e.g., $+10^{-5}$) per iteration. If the f_T exceeds 3.5 or the δ function at the current iteration is greater than that at the previous iteration, then the algorithm moves to the ω loop. The f_T value can be greater than the upper bound of 3.5 when MW_1 is much greater than the MW of benzene in eq 7. The accuracy of density predictions is less than 1% in AAD for all the oils tested in the next section.

$$\psi = \frac{\mathrm{abs}(\text{experimental } P_{SAT} - \text{calculated } P_{SAT})100}{\text{experimental } P_{SAT}} \tag{8}$$

$$\delta = \sum_{i=1}^{k} \frac{1}{k}\left[\frac{\mathrm{abs}(\text{experimental density} - \text{calculated density})100}{\text{experimental density}}\right]_i \tag{9}$$

The ω loop is to satisfy the internal consistency of T_C, P_C, and ω, that is, the definition of ω given by Pitzer[45] and Pitzer et al.[46] and in eq 10. Equations 11 and 12 are used to back calculate ω from the current m for each pseudocomponent. These ω values are then used in eq 10 to obtain saturation pressures for pseudocomponents (P_{SATI}) at $0.7T_C$.

$$(P_{SAT})_{\text{at } T_r=0.7} = 10^{-(1+\omega)} P_C \tag{10}$$

$$m = 0.37464 + 1.54226\omega - 0.26992\omega^2 \quad \text{for} \quad \omega \le 0.3984 \tag{11}$$

$$m = 0.379642 + 1.48503\omega - 0.164423\omega^2 + 0.016666\omega^3 \quad \text{for} \quad \omega \ge 0.3984 \tag{12}$$

Use of the PR EOS with the current T_C, P_C, and ω yields another saturation pressure at $0.7T_C$ (P_{SATII}) for each pseudocomponent. The average absolute deviation ε for P_{SATI} and P_{SATII} for all pseudocomponents is then calculated using eq 13

$$\varepsilon = \frac{1}{n}\sum_{i=1}^{n} \mathrm{Abs}(P_{SATI} - P_{SATII}) \tag{13}$$

where n is the number of pseudocomponents. If f_T is greater than 3.5 or the ε function at the current iteration is smaller than that at the previous iteration, f_m is increased by Δf_m (e.g., $+10^{-3}$) to continue on the ω loop. For each ω iteration, f_T and f_P start with 1.0. The final values for f_T, f_P, and f_m are determined when the ε function becomes greater than that at the previous iteration. The final set of f_T, f_P, and f_m gives the first minimum of the ε function encountered in the calculation.

In the regression algorithm, the initial value is 1.0 for f_T and f_P, corresponding to the n-alkane values in Kumar and Okuno.[51] The search direction for f_T and f_P is the increasing direction from their initial values because pseudocomponents' T_C and P_C should be higher than n-alkane's value for a given MW. Therefore, Δf_T and Δf_P are positive to be physically justified. We set a lower bound for f_m in eq 7, which is used as the initial f_m value. Thus, Δf_m should also be positive. If the converged f_m is smaller than 1.0, it is consistent with the ω perturbation concept that pseudocomponents' ω should be lower than n-alkane's value for a given MW.

The regression algorithm in the NM provides a unique set of T_C, P_C, and m unlike the CM, where the resulting T_C, P_C, and m depend on the selection of adjustment parameters and adjustment amounts for them. Our regression algorithm can work with fewer adjustment parameters, compared to the CM, because of the physical observations incorporated in its development.

Equations 11 and 12 are different from eqs 2 and 3 in terms of their ω ranges. Equations 2 and 3 give the same value for m at ω = 0.39839, but not at the boundary ω = 0.49. The value of 0.39839 falls in the ω range 0.20−0.49 that is recommended for both eqs 2 and 3 by Peng and Robinson.[9] Therefore, the value of 0.3984 is chosen as the boundary value for eqs 11 and 12.

In general, the PR EOS overpredicts the molar volume for hydrocarbons heavier than heptane (Søreide[56]). The values for the critical parameters must be increased to match densities and vapor pressures regardless of the hydrocarbon compound type

dx.doi.org/10.1021/ie402198z | Ind. Eng. Chem. Res. 2014, 53, 440−455

Table 1. Twenty Two Reservoir Oils Characterized in This Research and Converged f_T, f_P, and f_m Values Using the New Characterization Method

oil no.	refs	MW (gm/mol)	°API	reservoir temp. (K)	no. of density data (k in eq 9)	f_T	f_P	f_m
1	Quiñones-Cisneros et al.,[54] Oil-8	443.08	9.50	322.05	13	2.12110	1.74580	0.359
2	Quiñones-Cisneros et al.,[54] Oil-7	431.59	11.63	322.05	12	1.71016	1.65705	0.368
3	Quiñones-Cisneros et al.,[52] Oil-6	377.88	13.38	322.05	13	2.91379	1.83307	0.246
4	Quiñones-Cisneros et al.,[52] Oil-5	422.94	11.98	322.05	13	1.81952	1.67153	0.379
5	Quiñones-Cisneros et al.,[52] Oil-1	170.59	20.81	330.40	16	2.94230	1.78866	0.406
6	Quiñones-Cisneros et al.,[53] Oil-8	182.05	24.25	333.15	16	2.81319	1.91049	0.429
7	Quiñones-Cisneros et al.,[53] Oil-7	159.99	29.24	330.40	16	2.31276	1.74384	0.440
8	Quiñones-Cisneros et al.,[53] Oil-6	118.18	35.61	346.15	5	2.08100	1.71149	0.434
9	Quiñones-Cisneros et al.,[53] Oil-5	130.55	28.30	337.85	3	2.89841	1.84940	0.453
10	Quiñones-Cisneros et al.,[53] Oil-4	114.57	33.35	337.85	6	2.46282	1.74305	0.493
11	Quiñones-Cisneros et al.,[53] Oil-3	87.80	40.46	337.25	5	2.35278	1.64743	0.554
12	Quiñones-Cisneros et al.,[53] Oil-2	89.83	47.63	366.45	11	2.09759	1.47213	0.540
13	Quiñones-Cisneros et al.,[53] Oil-1	86.57	60.18	427.60	13	1.39453	1.18216	0.641
14	oil[a]	296.90	22.60[b]	357.50	13	2.19267	1.61825	0.309
15	Coats and Smart,[77] Oil-1	123.79	34.04	355.37	8	2.63596	1.84711	0.402
16	Coats and Smart,[77] Oil-6	83.31	55.73	385.37	20	2.06638	1.44575	0.453
17	Coats and Smart,[77] Oil-7	113.60	45.03	328.15	20	1.95919	1.47130	0.500
18	Quiñones-Cisneros et al.,[17] Oil-5	240.24	20.19	345.93	15	1.55725	1.57795	0.585
19	Quiñones-Cisneros et al.,[17] Oil-4	167.03	25.70	344.95	11	2.12027	1.68612	0.588
20	Quiñones-Cisneros et al.,[17] Oil-3	114.65	34.24	337.85	12	2.04203	1.60648	0.616
21	Cullick et al.,[78] Light Oil	105.28	43.68	377.59	8	1.99705	1.54570	0.414
22	Pedersen et al.,[32] Fluid-1	124.57	35.73	344.75	8	1.86796	1.54972	0.614

[a]This is an actual oil, but the source is not mentioned for confidentiality. [b]As reported. All other densities are calculated values.

(i.e., P or N or A). Also, the density of an aromatic hydrocarbon is higher than that of *n*-alkane for a given MW. Although the correlations used for *n*-alkanes do not represent physical critical points, the search directions described above are still valid as will be demonstrated in the next section.

The NM developed in this section uses the PR EOS. However, it can also be used with other cubic EOSs if a new set of critical parameters is developed for the selected cubic EOS as Kumar and Okuno[51] did for the PR EOS. The regression algorithm assumes that densities, viscosities, and P_{SAT} data are the only PVT data used in characterization. More adjustment parameters may be used when more PVT data are available, especially at different composition conditions. The regression algorithm can be extended for such a case by using molar distribution parameters as variables and creating additional loops. For example, the chi-squared distribution has two parameters, which influence mole fractions and MWs of pseudocomponents. These adjustment parameters will be effective especially for heavy oils, considering the importance of molar distributions of pseudocomponents in EOS calculations. BIPs for pseudocomponent/nonhydrocarbon (e.g., CO_2) pairs can significantly affect phase behavior calculations. We, however, recommend that the regression step should minimize the number of adjustment parameters to avoid physically absurd adjustment of parameters.

4. CHARACTERIZATION OF RESERVOIR OILS USING THE NEW METHOD

In this section, the NM is applied to 22 different reservoir oils ranging from 9.5°API to 60.18°API. The oils are actual reservoir oils, for which data are available in the literature as shown in Table 1. The number of pseudocomponents is fixed to be four for the 22 oils. Mole fractions and MWs of pseudocomponents for oils 1−13 and 18−20 are taken directly from the corresponding references, which are based on the chi-squared distribution. P_{SAT} and reservoir temperature data are available in the references as numerical values for the 22 oils. Many of the density data used have been obtained by digitizing density plots in the references. The number of density data points used is given for each oil in Table 1.

Figure 4 shows how the ε function varies with f_m for oils 5, 6, and 9. Step 4 of the NM converges to the final set of f_T, f_P, and f_m (and corresponding T_C, P_C, and m) at a minimum ε value for each oil. The same behavior of f_m occurs for the other oils studied in this research.

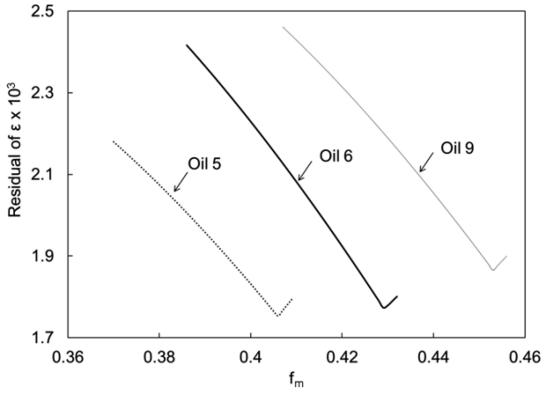

Figure 4. Convergence behavior for the ε function (eq 13) with f_m for oils 5, 6, and 9 given in Table 1. The regression algorithm (Figure S2 in the Supporting Information) finds an optimum set of f_T, f_P, and f_m at the minimum shown for each oil.

Table 1 lists the converged f_T, f_P, and f_m values for the 22 oils studied. Figures 5, 6, and 7 show the relationship between the API gravity and the converged f_T, f_P, and f_m values, respectively. For all the oils, the converged f_T and f_P values are greater than 1.0, and the converged f_m values are smaller than

dx.doi.org/10.1021/ie402198z | Ind. Eng. Chem. Res. 2014, 53, 440−455

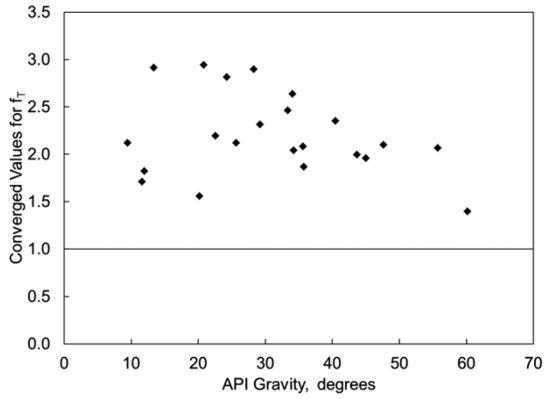

Figure 5. Converged f_T values for the 22 different oils in Table 1. The regression algorithm (Figure S2 in the Supporting Information) starts with f_T =1.0, and searches for an optimum f_T in the increasing direction. Perturbation of f_T from 1.0 qualitatively represents deviation of a plus fraction from an *n*-alkane mixture.

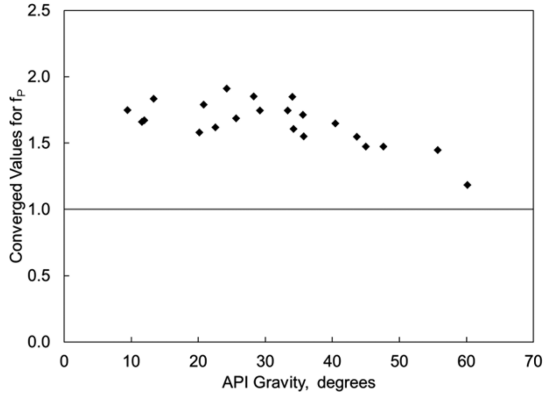

Figure 6. Converged f_P values for the 22 different oils in Table 1. The regression algorithm (Figure S2 in the Supporting Information) starts with f_P =1.0, and searches for an optimum f_P in the increasing direction. Perturbation of f_P from 1.0 qualitatively represents deviation of a plus fraction from an *n*-alkane mixture.

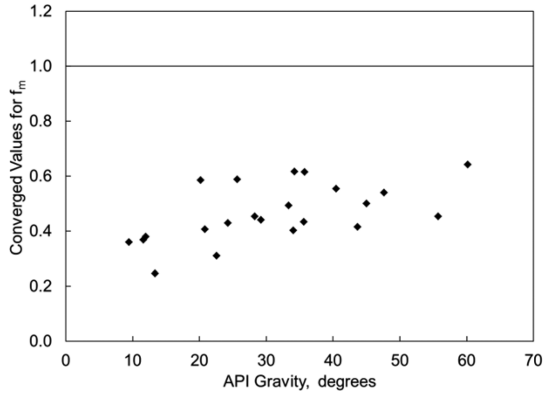

Figure 7. Converged f_m values for the 22 different oils in Table 1. The regression algorithm (Figure S2 in the Supporting Information) starts with f_m based on eq 7, and searches for an optimum f_m in the increasing direction. Perturbation of f_m from 1.0 qualitatively represents deviation of a plus fraction from an *n*-alkane mixture.

1.0. These results indicate that the regression algorithm successfully found the solutions that are consistent with the perturbation concept described in the previous section.

Figures 5−7 also show a trend that f_T, f_P, and f_m are converging toward 1.0 as the API gravity becomes larger. This is likely because the paraffinic portion of the PNA distribution for a lighter oil is greater than that for a heavier oil. The PNA distribution of a heavy oil in general can deviate significantly from the reference distribution of 100% *n*-alkanes because a heavier CN group allows for a wider variety of compounds in it.

Unlike manual adjustments performed in the CM, the regression process in the NM can be easily codified for automation and takes only 1−3 min per oil using our code written in FORTRAN on the Intel Core i7−960 processor at 3.20 GHz and 8.0 GB RAM. The algorithm presented is based on the exhaustive search method of optimization for robustness. More rapid convergence would be achieved if a gradient method is used with initial guesses for f_T, f_P, and f_m based on the previous iteration steps.

5. COMPARISON BETWEEN THE NEW AND CONVENTIONAL METHODS

We now make comparisons between the NM and CM in terms of various types of phase behavior predictions in *P-T-x* space for the oils in Table 1. PVT data for heavy oils are scarce as described in the introduction section and in the literature.[57,58] Data types used in this research are oil compositions, oil P_{SAT} at reservoir temperatures, and liquid densities and viscosities at different pressures at reservoir temperatures. Other than these measured data, pseudodata[59] were generated using the $CM_{w/o}V$ with 30 components (see Figure S1 in the Supporting Information) because a complete set of data suitable for comparisons in a wide *P-T-x* range is not available for heavy oils. The 30 components consist of N_2, CO_2, C_1, C_2, C_3, C_4, C_5, C_6, and 22 pseudocomponents for the C_{7+} fraction.

Fluid characterization using a cubic EOS can result in deviation between predictions and data for a few fundamental reasons: (1) the functional form of the EOS used, (2) the characterization of the attraction ("a") and covolume ("b") parameters based on critical parameters, (3) the critical parameters used, and (4) the number of components used. The focus of the comparisons in this section is on items 3 and 4. Thus, the comparisons are made among different fluid models that have different critical parameters and numbers of components for the PR EOS (i.e., for a fixed cubic EOS and a characterization method for a and b).

If the number of components in the fluid of interest was known and used in the fluid model, there should be no errors caused solely by reduction in composition space. We have conducted a sensitivity analysis for the effects of the number of components used on phase behavior predictions (Figures 8 and 9). The results indicate that use of 22 pseudocomponents is appropriate for generating pseudodata in this research. The differences in predictions are diminishing as the number of pseudocomponents used becomes more than 16. This result is consistent with other papers in the literature.[40,60,61] Also, the $CM_{w/o}V$ method used for generating pseudodata follows the method of Pedersen et al.[31−33] It has been found that this method generally has a high predictive capability[62] when properly used (see Figure S1 in the Supporting Information).

Given the above, the pseudodata generated can be interpreted as phase behavior data for a PR fluid, a fluid that behaves as described by the PR EOS. Global phase diagrams of binary (Mushrif,[63] Yang,[64] Mushrif and Phoenix[65]) and ternary (Gauter,[66] Gauter et al.[67]) mixtures have been successfully represented using the PR EOS. Their results show that the PR

dx.doi.org/10.1021/ie402198z | Ind. Eng. Chem. Res. 2014, 53, 440−455

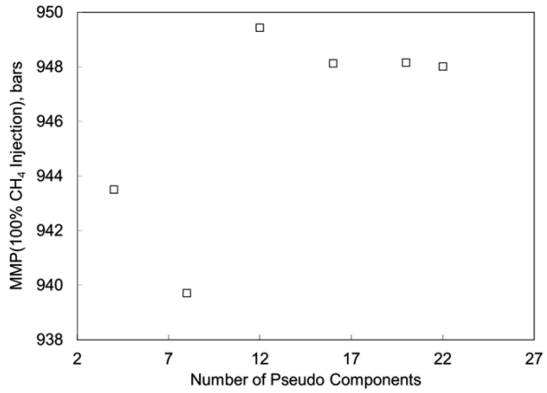

Figure 8. MMP calculated for Oil 6 with 100% methane at 333.15 K using $CM_{w/o}V$ with different numbers of pseudocomponents. Eight pure components (N_2, CO_2, C_1, C_2, C_3, C_4, C_5, and C_6) are used with 4, 8, 12, 16, 20, and 22 pseudocomponents. The variation of calculated MMP becomes insignificant for more than 16 pseudocomponents.

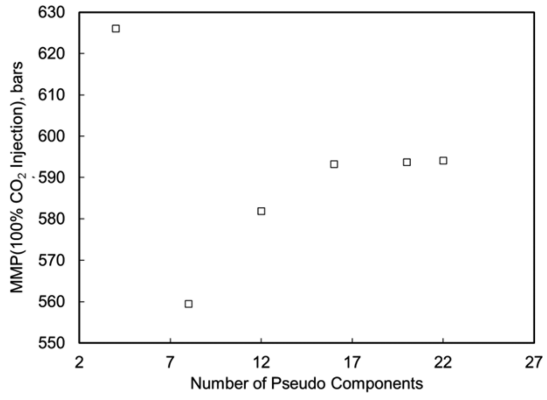

Figure 9. MMP calculated for Oil 6 with 100% CO_2 at 333.15 K using $CM_{w/o}V$ with different numbers of pseudocomponents. Eight pure components (N_2, CO_2, C_1, C_2, C_3, C_4, C_5, and C_6) are used with 4, 8, 12, 16, 20, and 22 pseudocomponents. The variation of calculated MMP becomes insignificant for more than 16 pseudocomponents.

EOS is capable of predicting at least qualitatively accurate phase behavior for reservoir fluids. When experimental data are not available or measurable, use of synthetic or pseudodata has been recommended for developing thermodynamic fluid models (Satyro et al.[68]). In the present research, the validation of the NM is made against pseudodata for PR fluids. We believe this is a reasonable approach in the absence of reliable experimental data other than oil compositions, densities, saturation pressures, and viscosities. There is also an important benefit using the pseudodata. Meaningful comparisons in any conditions in *P-T-x* space, particularly along the composition path for a given displacement at a given dispersion level, may be possible only with the pseudodata.

Separately from the 30-component models created for pseudodata, two fluid models are created for each oil using the NM and CM_wV with 11 components (see Figures S1 and S2 in the Supporting Information for the CM_wV and NM algorithms, respectively). The 11 components consist of N_2, CO_2, C_1, C_2, C_3, C_{4-5}, C_6, and four pseudocomponents for the C_{7+} fraction.

BIPs are not adjustment parameters in this research. Fixed BIP values are used for the 22 oils. BIPs are zero for hydrocarbon-hydrocarbon pairs. Nonzero values are used for nonhydrocarbon−hydrocarbon and nonhydrocarbon−nonhydrocarbon pairs, that is, N_2−hydrocarbons, CO_2−hydrocarbons, and N_2−CO_2.

We adjust no BIPs and set BIPs of hydrocarbon-hydrocarbon pairs to zero for the following reasons:

(1) The number of regression parameters should be minimized (Wang and Pope;[39] Egwuenu et al.[60]). Use of BIPs as regression parameters can damage the predictive capability of the resulting fluid model (Wang and Pope[39]).
(2) Nonzero BIPs for hydrocarbon-hydrocarbon pairs may lead to nonphysical liquid-phase split (Pedersen et al.[69]).
(3) Use of zero BIPs can improve computational efficiency (Egwuenu et al.;[60] Michelsen[70]). It has also been shown that fluid properties can be better predicted when most of BIPs are set to zero (Pedersen and Christensen[15]).
(4) Use of negative BIPs, which may occur after regression, can cause nonconvergence in successive substitution for flash calculations (Heidemann and Michelsen[71]).

The BIPs for N_2-hydrocarbons, CO_2-hydrocarbons, and N_2−CO_2 are fixed to be some nonzero values. The CM uses the default values from PVTsim as they would be the most suitable values for PVTsim. They are −0.017 for N_2−CO_2, 0.0311 for N_2−C_1, 0.0515 for N_2−C_2, 0.0852 for N_2−C_3, 0.08 for N_2−C_4, 0.1 for N_2−C_5, 0.08 for N_2−C_i, where $i \geq 6$, 0.12 for CO_2,−C_j, where $1 \leq j \leq 6$, and 0.1 for CO_2-pseudocomponents. These BIPs in the NM are based on Peng and Robinson,[8,9] who properly considered effects of hydrocarbon types on BIPs for the PR EOS. They recommended 0.1 for N_2-paraffins and N_2-napthenes, 0.18 for N_2-aromatics, and 0.1 for CO_2-hydrocarbons. Since pseudocomponents are mixtures of PNA compounds, we use the average values in the NM, which is $[0.1 + 0.1 + 0.18]/3 = 0.12666 \approx 0.13$ for N_2-pseudocomponents, and 0.1 for CO_2-pseudocomponents. The NM uses 0.0 for N_2−CO_2, 0.1 for N_2−C_i, where $1 \leq i \leq 6$, 0.13 for N_2-pseudocomponents, and 0.1 for CO_2-hydrocarbons.

In the following subsections, phase behavior predictions based on the NM and CM_wV are compared with the pseudodata. Tables S1, S2, S3, and S4 (in the Supporting Information) give the resulting fluid models for oil 3 (13.38°API) and oil 6 (24.25°API) using the NM and CM_wV. These models are used in many of the comparisons presented below.

5.1. *P*−*T* Predictions. We first present the comparisons in terms of *P*−*T* predictions. Heavy-oil/solvent mixtures often exhibit three hydrocarbon-phases near the vapor pressures of the solvent components. The three phases consist of the gaseous (V), oleic (L_1), and solvent-rich liquid (L_2) phases (e.g., Mohanty et al.;[1] Polishuk et al.[37]). Figures 10 and 11 show the 2-phase and 3-phase envelopes for a mixture of 10% oil 6 and 90% C_2. The CM_wV gives the V−L_1 and V−L_1−L_2 regions that are much smaller than those predicted by the NM. The NM predictions are in good agreement with the pseudodata points. The NM predictions are more accurate for lower temperatures. The three-phase envelope predicted by the NM almost coincides with data.

The deviation of the CM_wV predictions from the pseudodata is more significant for a mixture of 10% oil 6 and 90% C_3. Figure 12 shows that the CM_wV results in an erroneous two-phase envelope for this mixture. The NM correctly generates the phase behavior predictions. Figure 13 shows that the NM predicts a three-phase envelope that is close to the data points. The three-phase behavior predicted by the CM_wV occurs in a

dx.doi.org/10.1021/ie402198z | Ind. Eng. Chem. Res. 2014, 53, 440−455

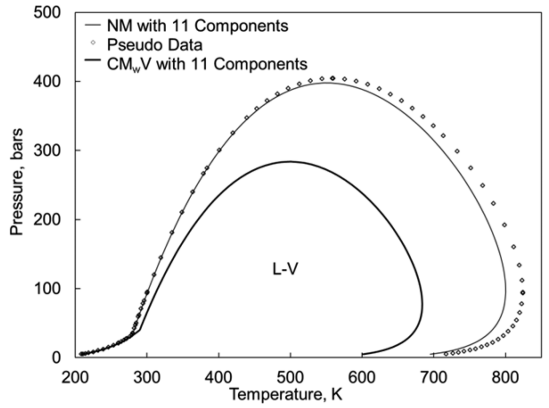

Figure 10. Two-phase $P-T$ diagrams for a mixture of oil 6 10% and C_2 90% based on the new characterization method (NM) and the conventional characterization method with volume-shift parameters (CM_wV). The 11-component models for oil 6 are given in Tables S3 and S4 in the Supporting Information. The pseudodata are generated using the conventional method without using volume shift parameters ($CM_{w/o}V$) with 30 components.

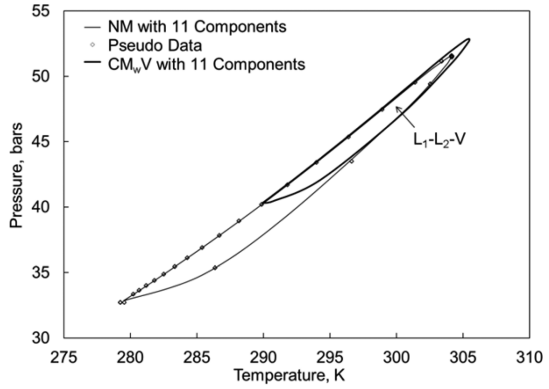

Figure 11. Three-phase $P-T$ diagrams for a mixture of oil 6 10% and C_2 90% based on the NM and the CM_wV. The 11-component models for oil 6 are given in Tables S3 and S4 in the Supporting Information. The pseudodata are generated using the $CM_{w/o}V$ with 30 components.

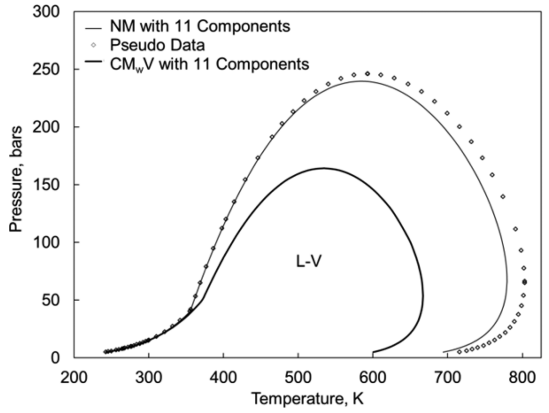

Figure 12. Two-phase $P-T$ diagrams for a mixture of oil 6 10% and C_3 90% based on the NM and the CM_wV. The 11-component models for oil 6 are given in Tables S3 and S4 in the Supporting Information. The pseudodata are generated using the $CM_{w/o}V$ with 30 components.

much smaller $P-T$ region apart from the correct three-phase region based on the pseudodata and the NM.

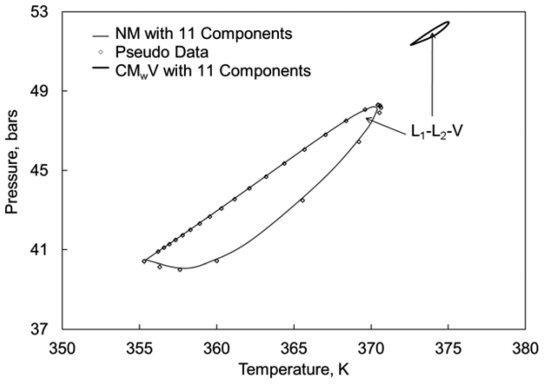

Figure 13. Three-phase $P-T$ diagrams for a mixture of oil 6 10% and C_3 90% based on the NM and the CM_wV. The 11-component models for oil 6 are given in Tables S3 and S4 in the Supporting Information. The pseudodata are generated using the $CM_{w/o}V$ with 30 components.

The accuracy of the NM for L_1-L_2-V phase behavior is remarkable considering that the complex phase behavior characteristic of highly asymmetric hydrocarbon mixtures is predicted using only four pseudocomponents for the C_{7+} fraction. The reduced dimensionality in composition space does not damage phase behavior predictions using the NM.

5.2. *P–x* Predictions. A $P-x$ prediction presents a cross section of isothermal phase behavior between two compositions. This subsection shows $P-x$ predictions for the oil-6/C_1, oil-6/C_2, and oil-6/CO_2 pairs at the oil-6 reservoir temperature 333.15 K. Figure 14 shows the $P-x$ predictions along with

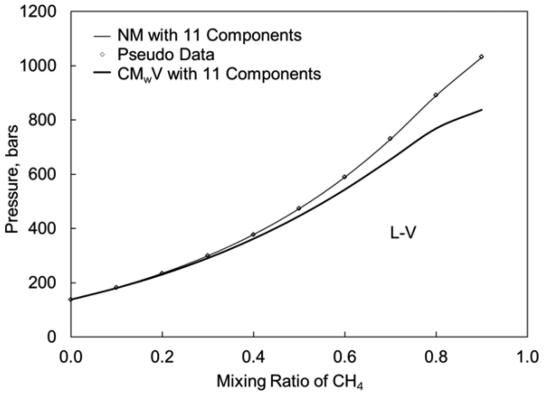

Figure 14. $P-x$ diagrams for the oil-6/C_1 pseudobinary pair at 333.15 K based on the NM and CM_wV with 11 components. The 11-component models are given in Tables S3 and S4 in the Supporting Information. The pseudodata are generated using the $CM_{w/o}V$ with 30 components.

pseudodata for the oil-6/C_1 pair. The NM and CM_wV are accurate at low mixing ratios of C_1. This is because the 11-component models are fitted to P_{SAT} at the reservoir temperature at the oil composition. As the mixture composition goes away from the oil composition, the CM_wV predictions deviate from the pseudodata. The NM accurately predicts the bubble-point pressures along the mixing line.

The advantage of the NM over the CM_wV becomes more significant for $P-x$ predictions for the oil-6/C_2 pair as shown in Figure 15. At the C_2 mixing ratio of 90%, the CM_wV predicts a bubble point at 137.44 bar, which is approximately 39 bar lower than the pseudodata and the prediction by the NM.

dx.doi.org/10.1021/ie402198z | Ind. Eng. Chem. Res. 2014, 53, 440−455

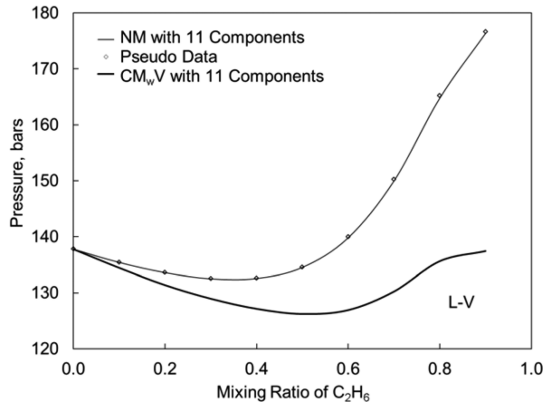

Figure 15. $P-x$ diagrams for the oil-6/C_2 pseudobinary pair at 333.15 K based on the NM and CM_wV with 11 components. The 11-component models are given in Tables S3 and S4 in the Supporting Information. The pseudodata are generated using the $CM_{w/o}V$ with 30 components.

Mixtures of CO_2 and reservoir oil often exhibit continuous transition between L_1-V and L_1-L_2 phase equilibria (Okuno et al.[72]) at low temperatures. Figure 16 presents such phase

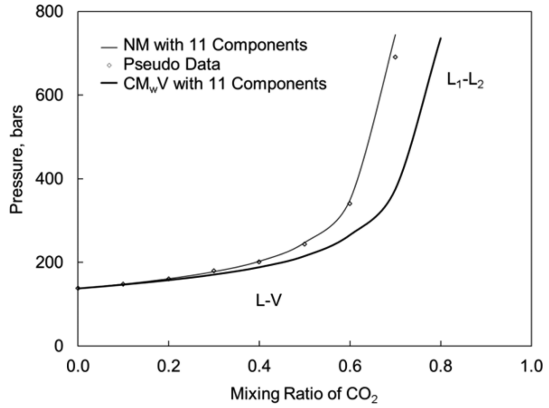

Figure 16. $P-x$ diagrams for the oil-6/CO_2 pseudobinary pair at 333.15 K based on the NM and CM_wV with 11 components. The 11-component models are given in Tables S3 and S4 in the Supporting Information. The pseudodata are generated using the $CM_{w/o}V$ with 30 components.

behavior for oil 6 and CO_2 at 333.15 K. The NM accurately predicts the upper boundary of the two-phase region in $P-x$ space. The CM_wV erroneously gives a smaller region for the immiscible two liquid phases.

Figure 17 shows saturated liquid densities predicted along the mixing line between oil 6 and the equimolar C_1-C_2 mixture at 333.15 K. The density at the oil composition was used to create the EOS fluid models. Therefore, the CM_wV and NM are both accurate at lower mixing ratios of the solvent. As the mixture composition goes away from the oil composition, however, the CM_wV predictions deviate from the NM predictions and the pseudodata. The results indicate that the fluid models based on the CM_wV cannot accurately represent phase equilibrium and volumetric properties at compositions away from the oil composition.

5.3. $T-x$ Predictions. A $T-x$ diagram presents another important cross section of phase behavior, particularly when coinjection of solvent and steam is considered for heavy-oil recovery. Figure 18 shows $T-x$ predictions for oil-3/C_6

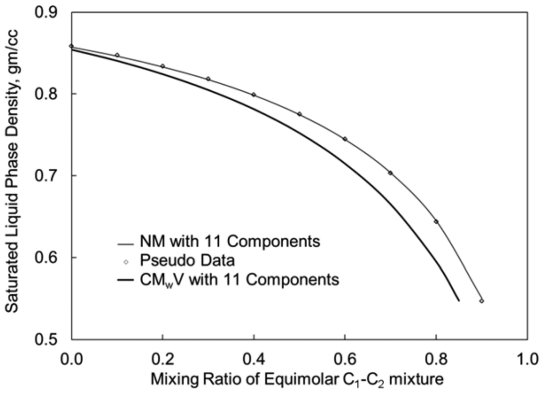

Figure 17. Saturated liquid densities for mixtures of oil 6 and the equimolar C_1-C_2 mixture at 333.15 K. The 11-component models based on the NM and the CM_wV are given in Tables S3 and S4 in the Supporting Information, respectively. The pseudodata are generated using the $CM_{w/o}V$ with 30 components.

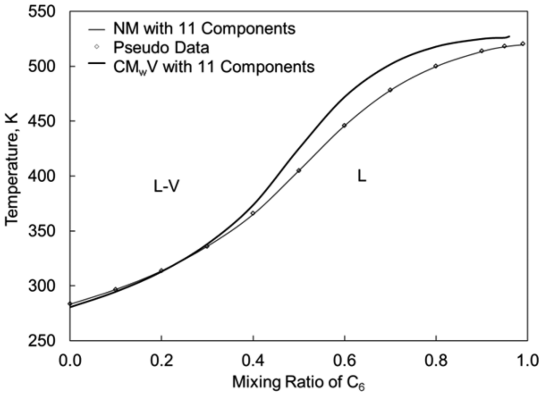

Figure 18. $T-x$ diagrams for the oil-3/C_6 pseudobinary pair at 34.47 bar. The 11-component models based on the NM and the CM_wV are given in Tables S1 and S2 in the Supporting Information, respectively. The pseudodata are generated using the $CM_{w/o}V$ with 30 components.

mixtures at 34.47 bar. The CM_wV overpredicts saturation temperatures except for low C_6 mixing ratios, while the NM accurately predicts them along the mixing line. If the fluid model based on the CM_wV is used in reservoir simulation of solvent/steam coinjection, propagation of the solvent in the reservoir can be significantly underestimated, resulting in erroneous reservoir performance forecasts.

The overprediction of saturation temperatures by the CM_wV becomes more significant for higher pressures. Figure 19 shows $T-x$ predictions at 60.00 bar. The NM still predicts accurately the saturation temperatures at all mixing ratios tested. However, the CM_wV predicts much higher saturation temperatures even at low C_6 mixing ratios. The deviation at the C_6 mixing ratio of 0.3 is 139 K. At C_6 mixing ratios higher than 0.3, there are no saturation temperatures predicted by CM_wV because the cricondenbar becomes lower than 60.00 bar as can be seen in Figure 20.

5.4. Thermodynamic Minimum Miscibility Pressure (MMP) Calculation. The thermodynamic MMP is the minimum displacement pressure at which complete miscibility is developed along the composition path from the injectant to the reservoir oil for one-dimensional flow in the absence of dispersion.[73] The thermodynamic MMP is a widely used parameter for design of solvent injection. In this subsection, the

dx.doi.org/10.1021/ie402198z | Ind. Eng. Chem. Res. 2014, 53, 440−455

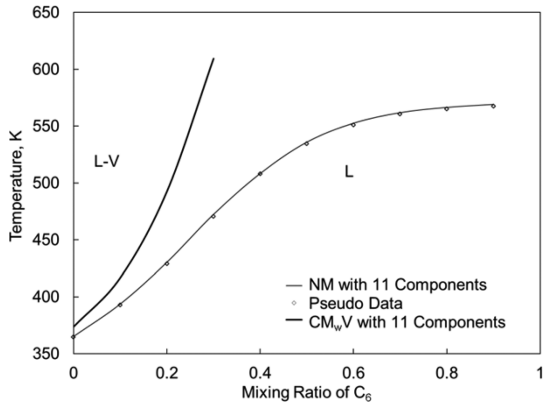

Figure 19. $T-x$ diagrams for the oil-3/C_6 pseudobinary pair at 60.00 bar. The 11-component models based on the NM and the CM_wV are given in Tables S1 and S2 in the Supporting Information, respectively. The pseudodata are generated using the $CM_{w/o}V$ with 30 components.

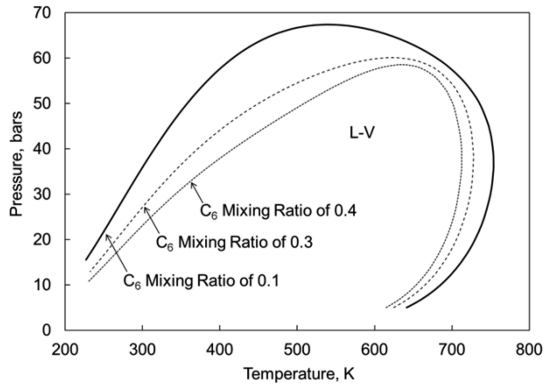

Figure 20. Two-phase $P-T$ diagrams for mixtures of oil 3 and C_6 at four different C_6 mixing ratios, 0.1, 0.3, and 0.4. At the C_6 mixing ratio of 0.4, there is no two-phase region at 60.0 bar, which can be also seen in Figure 17

thermodynamic MMPs are calculated for 18 oils in Table 1 at their reservoir temperatures. Two different injectants are considered: pure C_1 and pure CO_2. For the C_1 cases, the MMP calculations are performed based on the method of characteristics using PVTsim. For the CO_2 cases, the mixing-cell method within PennPVT[74,75] is used. MMP calculations are not shown for oils 1, 2, 4, and 18 because three phases are present during the MMP calculations using the EOS fluid models for these oils based on the $CM_{w/o}V$ with 30 components.

Figure 21 compares the MMPs based on the NM with the pseudodata for 18 oils with C_1. Although the C_1-MMPs presented are calculated at different temperatures, the plots show that the calculated C_1-MMPs are higher for heavier oils. The accuracy of the MMPs observed for the wide variety of oils indicates that the NM successfully retains compositional phase behavior using only four pseudocomponents for the C_{7+} fraction. Figure 22 shows that the C_1-MMPs predicted based on the CM_wV are lower than the pseudodata. The deviation is more significant for heavier oils. The maximum deviation of the C_1-MMPs is 5.3% for the NM, but it is 34% for the CM_wV. Figures 23 and 24 show the comparisons of the NM with the CM_wV in terms of the CO_2-MMP. The maximum deviations of the CO_2-MMPs are 6.1% and 62% for the NM and the CM_wV, respectively.

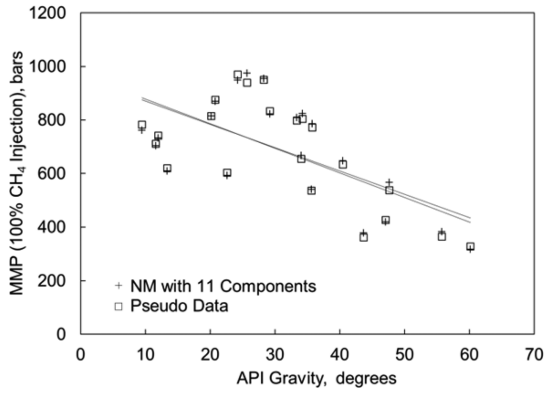

Figure 21. Comparison of MMP calculations for 22 oils in Table 1 based on the NM with 11 components and the $CM_{w/o}V$ with 30 components. The injection gas is pure methane. The MMPs for 18 oils are calculated at their own reservoir temperatures, which are different from one another. The two trend lines for the NM with 11 components and the $CM_{w/o}V$ with 30 components almost overlap each other.

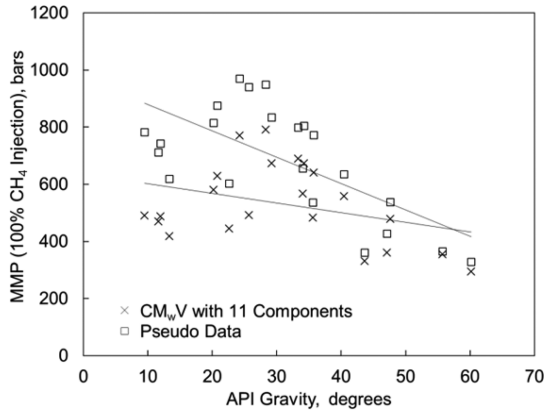

Figure 22. Comparison of MMP calculations for 22 oils in Table 1 based on the CM_wV with 11 components and the $CM_{w/o}V$ with 30 components. The injection gas is pure methane. The MMPs for 18 oils are calculated at their own reservoir temperatures, which are different from one another. The two trend lines for the CM_wV with 11 components and the $CM_{w/o}V$ with 30 components deviate from each other as the API gravity becomes smaller.

Figures 22 and 24 indicate that compositional phase behavior predictions are more erroneous for heavier oils using the CM_wV. This is because the CM_wV uses density corrections through volume shift parameters. A larger amount of volume correction is required and performed for heavier oils in the CM_wV as shown in Tables S2 and S4 in the Supporting Information (see also the Issues of the Conventional Method subsection). However, the thermodynamic MMP considered here is a parameter representing primarily compositional phase behavior, instead of volumetric phase behavior, of the fluid system considered. Therefore, the separation of volumetric from compositional phase behavior predictions causes errors in MMP predictions.

5.5. 1-D Displacement Simulation Case Study. Solvent injection for heavy-oil recovery is typically conducted under partially miscible conditions. In such displacements, the oil recovery history depends on how components propagate with the throughput of injectant. Fluid characterization can significantly affect oil recovery predictions because interaction

dx.doi.org/10.1021/ie402198z | Ind. Eng. Chem. Res. 2014, 53, 440−455

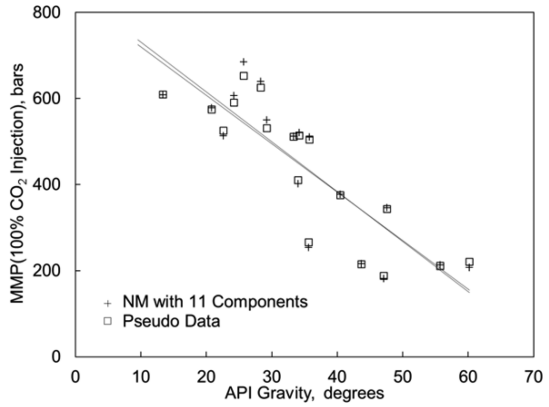

Figure 23. Comparison of MMP calculations for 18 oils in Table 1 based on the NM with 11 components and the $CM_{w/o}V$ with 30 components. The injection gas is pure CO_2. The MMPs for 18 oils are calculated at their own reservoir temperatures, which are different from one another. The two trend lines for the NM with 11 components and the $CM_{w/o}V$ with 30 components are close to each other.

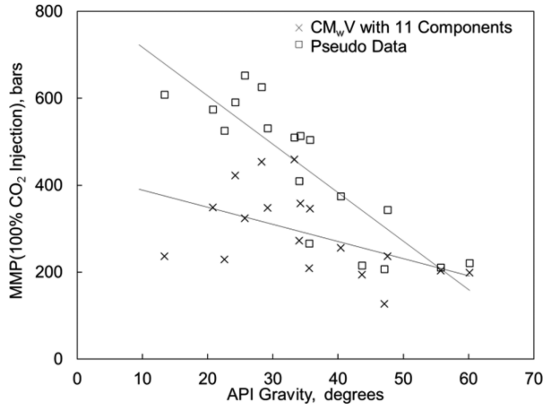

Figure 24. Comparison of MMP calculations for 18 oils in Table 1 based on the CM_wV with 11 components and the $CM_{w/o}V$ with 30 components. The injection gas is pure CO_2. The MMPs for 18 oils are calculated at their own reservoir temperatures, which are different from one another. The two trend lines for the CM_wV with 11 components and the $CM_{w/o}V$ with 30 components deviate from each other as the API gravity becomes smaller.

of phase behavior and fluid flow determines components' propagation in a reservoir. This simulation case study aims to compare predictions of components' propagation using the NM and CM.

We present 1-D isothermal displacement of oil 6 with the equimolar C_1/C_2 mixture under partially miscible conditions. The MMP calculated for this case is 412.23 bar using the $CM_{w/o}V$ with 30 components. Using 11 components, it is 413.34 bar and 327.23 bar based on the NM and the CM_wV, respectively (see Tables S3 and S4 in the Supporting Information for the fluid models). Input data for the simulations using the GEM simulator of Computer Modeling Group[76] are given in Table 2. Figures 25 and 26 present predictions of density and viscosity using the NM, CM_wV, and $CM_{w/o}V$, along with experimental data. Viscosity was matched using PVTsim by adjusting only V_C of pseudocomponents using the LBC method.[44] The injection and production pressures are fixed at 203.45 bar and 200 bar, respectively. The small pressure difference is used to make pressure variation in the reservoir small. Simulation results based on the $CM_{w/o}V$

Table 2. Input Parameters Used in the 1-D Simulation Case Study

no. of gridblocks	250	reservoir pressure	200 bar
grid dimensions	3.05 m × 3.05 m × 1.52 m	reservoir temp.	333.15 K
permeability	1500 mD	production pressure	200 bar
porosity	0.15	injection pressure	203.45 bar
initial oil saturation	0.8		
initial water saturation	0.2	injection gas	CH_4:C_2H_6 (50:50)

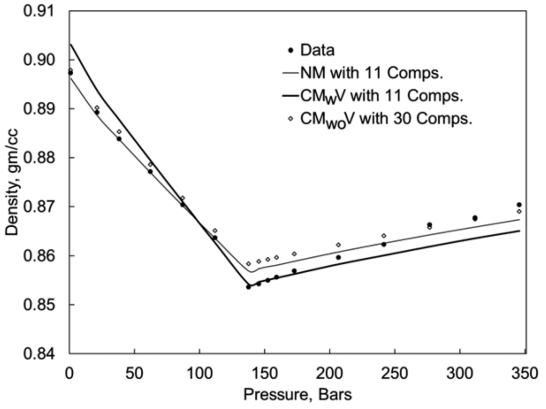

Figure 25. Measured and calculated densities for oil 6 at 333.15 K. Adjustment of pseudocomponents' T_C, P_C, and ω is performed for the NM with 11 components, and the $CM_{w/o}V$ with 30 components. The CM_wV with 11 components adjusts only volume shift parameters of pseudocomponents to match densities.

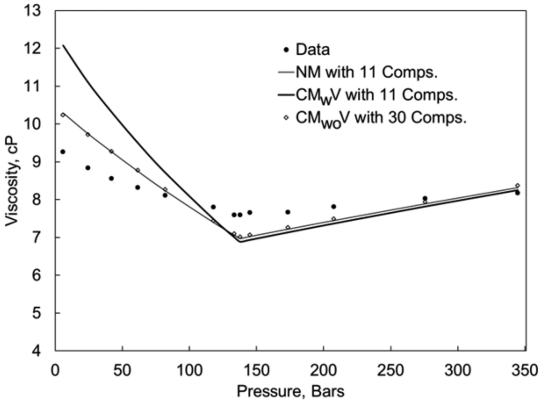

Figure 26. Measured and calculated viscosities for oil 6 at 333.15 K. Adjustment of V_C was performed for pseudocomponents to match viscosities using the LBC method for the NM and CM_wV with 11 components, and the $CM_{w/o}V$ with 30 components.

with 30 components are used as pseudodata. Simulation results based on the NM and CM_wV are then compared.

Figure 27 shows oil recovery predictions compared to the pseudodata. The recovery curves for 0.0−0.3 hydrocarbon pore-volumes injected (HCPVI) are not shown because they nearly coincide. Oil recovery based on the NM is almost identical to the pseudodata. However, the CM_wV results in oil recovery simulation that is significantly overpredicted by approximately 8%. The overprediction is consistent with other comparisons made in previous subsections, where the

dx.doi.org/10.1021/ie402198z | Ind. Eng. Chem. Res. 2014, 53, 440−455

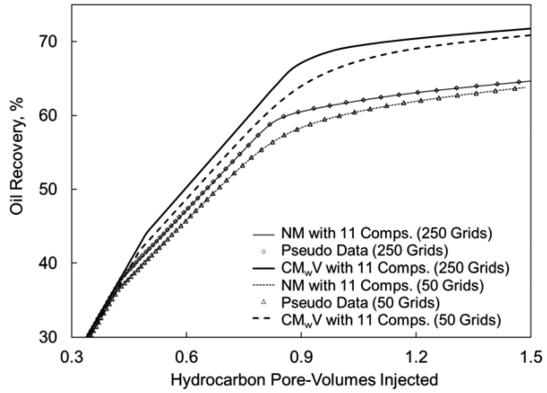

Figure 27. Oil recovery predictions in 1-D oil displacement simulations based on the NM and CM_wV with 11 components, along with pseudodata points generated from the $CM_{w/o}V$ with 30 components. Oil 6 is displaced by the equimolar C_1/C_2 mixture at 333.15 K at 200 bar, which is below MMP. Input parameters are given in Table 2. The recovery curves for 0.0−0.3 HCPVI nearly coincide, and they are not shown.

fluid models based on the CM_wV exhibit more miscibility in their phase diagrams and MMP calculations. To see the effect of numerical dispersion on oil recovery simulation, the number of gridblocks is decreased from 250 to 50. Figure 27 shows the same advantage of the NM over the CM_wV under more dispersive conditions (The previous subsection showed comparisons for the dispersion-free case). The number of gridblocks is fixed to be 250 for further comparisons.

The different oil recovery histories are predicted because the NM and CM_wV predict different saturation profiles as shown in Figure 28. Figure 29 shows that the C_1 fronts based on the NM

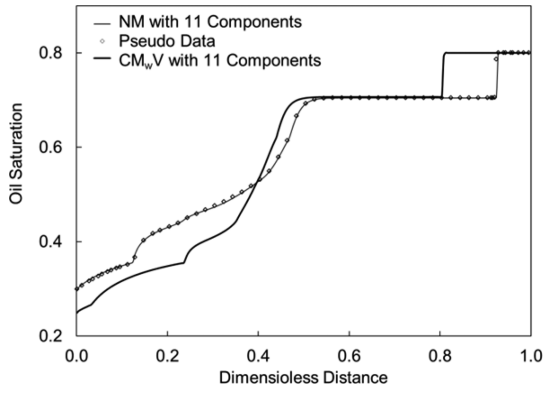

Figure 28. Oil saturation profiles at 0.4 HCPVI for the oil-6 displacement with the equimolar C_1/C_2 mixture at 333.15 K and 200 bar. Predictions using the NM and CM_wV with 11 components are shown along with pseudodata generated from the $CM_{w/o}V$ with 30 components.

and CM_wV deviate from each other, resulting in different predictions of gas breakthrough as can be seen in Figure 27. Figure 28 also indicates the CM_wV erroneously predicts faster propagation of heavy components. Since the deviation of the CM_wV shown in Figure 28 increases with the injectant throughput, the simulation based on the CM_wV becomes more erroneous at later times.

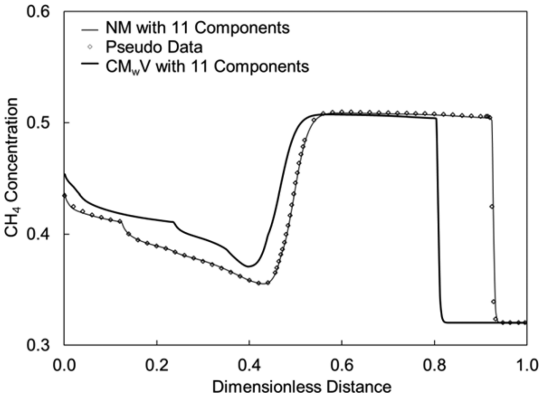

Figure 29. Concentration profiles for C_1 at 0.4 HCPVI for the oil-6 displacement with the equimolar C_1/C_2 mixture at 333.15 K and 200 bar. Predictions using the NM and CM_wV with 11 components are shown along with pseudodata generated from the $CM_{w/o}V$ with 30 components.

6. CONCLUSIONS

We developed a new method for fluid characterization using the PR EOS with the van der Waals mixing rules. The method characterizes reservoir fluids using perturbations of T_C, P_C, and ω from *n*-alkane values. T_C, P_C, and ω for *n*-alkanes used are based on our previous research, which are optimized for the PR EOS for predictions of vapor pressures and liquid densities without volume shift. The optimized reference values allow for robust regression using three perturbation factors f_T, f_P, and f_m for T_C, P_C, and ω, respectively. In our regression, Pitzer's definition of ω is properly satisfied for each component. The new characterization method was applied to 22 different reservoir oils. Comparisons were made between the new and conventional characterization methods in terms of predictions of various phase diagrams, thermodynamic minimum miscibility pressures (MMPs), and 1-D oil displacement. The conclusions are as follows:

- The new method (NM) exhibits significant insensitivity of phase behavior predictions to the number of components used for a plus fraction. Two- and three-phase behavior predictions in *P-T-x* space using the NM with 11 components are almost identical to those using the conventional method without volume shift ($CM_{w/o}V$) with 30 components.
- The reliability of the NM is also observed for MMP calculations and 1-D oil displacement simulations. Oil displacement predictions based on the NM with 11 components are nearly identical to those based on the $CM_{w/o}V$ with 30 components. This is true even at different dispersion levels tested. Results indicate that the NM can reduce the dimensionality of composition space while keeping accurate phase behavior predictions along composition paths at different dispersion levels.
- The NM does not require volume shift parameters to accurately predict compositional and volumetric phase behaviors. The conventional method with volume shift (CM_wV) separates volumetric phase behavior predictions from compositional phase behavior predictions. This separation should be carefully used especially for heavy-oil characterization. Our results show that the CM_wV with 11 components yields erroneous phase behavior predictions, which typically show significantly smaller

dx.doi.org/10.1021/ie402198z | *Ind. Eng. Chem. Res.* 2014, 53, 440−455

two- and three-phase regions in *P-T-x* space. The advantage of the NM over the CM_wV in phase behavior predictions is more significant for *P-T-x* conditions away from those used for parameter regression.

- The new regression algorithm developed searches for an optimum set of T_C, P_C, and ω for pseudocomponents using physically justified search directions starting from the well-defined initial values. Unlike in the CM, robust convergence of T_C, P_C, and ω does not require stepwise manual adjustments of parameters. The automatic regression process in the NM took only a few minutes per oil for the 22 oils characterized.
- The perturbation factors f_T, f_P, and f_m developed in this research are unity for *n*-alkanes. The perturbation factors capture physical trends that can be derived from the literature; for example, for a given molecular weight, T_C and P_C are lower and ω is larger for paraffins compared to other types of hydrocarbon compounds. For the 22 oils characterized in this research, the converged f_T and f_P values are all greater than 1.0, and the converged f_m values are all smaller than 1.0. Deviations of f_T, f_P, and f_m from unity can be physically interpreted as deviations of the plus fractions from *n*-alkane mixtures.
- The NM requires no changes in the current compositional simulation formulation because it uses the PR EOS with the van der Waals mixing rules.

■ ASSOCIATED CONTENT

Supporting Information

Tables S1−S5, Figures S1−S6, and sections S1 and S2. This material is available free of charge via the Internet at http://pubs.acs.org.

■ AUTHOR INFORMATION

Corresponding Author

*Phone: +1-780-492-6121. Fax: +1-780-492-0249. E-mail: rokuno@ualberta.ca.

Notes

The authors declare no competing financial interest.

■ ACKNOWLEDGMENTS

This research was funded by research grants from the Natural Sciences and Engineering Research Council of Canada (RGPIN 418266) and Japan Petroleum Exploration Co., Ltd. (JAPEX). Ashutosh Kumar was awarded the Union Pacific Resources Inc. Graduate Scholarship in Petroleum Engineering at the University of Alberta. Ryosuke Okuno was awarded the SPE Petroleum Engineering Junior Faculty Research Initiation Award. We gratefully acknowledge these supports. We also thank Dr. Russell T. Johns for providing the PennPVT software.

■ NOMENCLATURE

Roman Symbols

a = attraction parameter in a cubic equation of state
A = aromatic
A_{mix} = attraction parameter for a mixture in a cubic equation of state
b = covolume parameter in a cubic equation of state
B_{mix} = covolume parameter for a mixture in a cubic equation of state
C_{PEN} = Peneloux volume-shift parameter
m = parameter in the Peng−Robinson EOS (1978) defined in eqs 2 and 3
D = dimension
f_m = perturbation factor for the m parameter
f_P = perturbation factor for critical pressure
f_T = perturbation factor for critical temperature
Δf_m = step size for f_m
Δf_P = step size for f_P
Δf_T = step size for f_T
m_A = m parameter for aromatics
k = number of density data
m_P = m parameter for paraffins
n = number of pseudocomponents
N = napthenes
p = pressure, bar
P = paraffins
P_C = critical pressure, bar
P_{CA} = critical pressure of aromatics, bar
P_{CP} = critical pressure of paraffins, bar
R = universal gas constant
T = temperature, K
T_C = critical temperature, K
T_{CA} = critical temperature of aromatics, K
T_{CP} = critical temperature of paraffins, K
TOL = tolerance
υ = molar volume, gm/mol
V_C = critical volume, gm/mol

Abbreviations

°API = API (American Petroleum Institute) gravity
BIP = binary interaction parameter
CM = conventional (characterization) method
CM_wV = conventional (characterization) method using volume shift
$CM_{w/o}V$ = conventional (characterization) method without using volume shift
CN = carbon number
EOR = enhanced oil recovery
EOS = equation of state
HCPVI = hydrocarbon pore-volume injected
MMP = minimum miscibility pressure, bar
MW = molecular weight, gm/mol
NM = new (characterization) method
PC = pseudocomponent
PNA = paraffin−napthene−aromatic
PR = Peng−Robinson
P-T-x = pressure−temperature−composition
SRK = Soave−Redlich−Kwong

Greek Symbols

δ = average absolute deviation for density given by eq 9
ε = average absolute deviation for saturation pressure given by eq 13
Ω_a = constant term in the attraction parameter of a cubic EOS
Ω_b = constant term in the covolume parameter of a cubic EOS
ψ = absolute % deviation given by eq 8
ω = acentric factor

■ REFERENCES

(1) Mohanty, K. K.; Masino, W. H., Jr.; Ma, T. D.; Nash, L. J. Role of Three-Hydrocarbon-Phase Flow in a Gas-Displacement Process. *SPE Res. Eng.* **1995**, *10*, 214.

(2) DeRuiter, R. A.; Nash, L. J.; Singletary, M. S. Solubility and Displacement Behavior of a Viscous Crude with CO_2 and Hydrocarbon Gases. *SPE Res. Eng.* **1994**, *9*, 101.
(3) Hornbrook, M. W.; Dehghani, K.; Qadeer, S.; Ostermann, R. D.; Ogbe, D. O. Effects of CO_2 Addition to Steam on Recovery of West Sak Crude Oil. *SPE Res. Eng.* **1991**, *6*, 278.
(4) Nasr, T. N.; Beaulieu, G.; Golbeck, H.; Heck, G. Novel Expanding Solvent-SAGD Process "ES-SAGD". *J. Can. Pet. Technol.* **2003**, *42*, 13.
(5) Gupta, S.; Gittins, S.; Picherack, P. Insights into Some Key Issues with Solvent Aided Process. *J. Can. Pet. Technol.* **2003**, *43*, 54.
(6) Li, W.; Mamora, D. D.; Li., Y. Solvent-Type and -Ratio Impacts on Solvent-Aided SAGD Process. *SPE Reservoir Eval. Eng.* **2011**, *14*, 320.
(7) Gates, I. D.; Chakrabarty, N. Design of the Steam and Solvent Injection Strategy in Expanding Solvent Steam-Assisted Gravity Drainage. *J. Can. Pet. Technol.* **2008**, *47*, 12.
(8) Peng, D.-Y.; Robinson, D. B. A New Two-Constant Equation of State. *Ind. Eng. Chem. Fundam.* **1976**, *15*, 59.
(9) Peng, D.-Y.; Robinson, D. B. *The Characterization of the Heptanes and Heavier Fractions for the GPA Peng−Robinson Programs*; GPA Research Report RR-28; Gas Processors Association: Tulsa, OK, 1978.
(10) Soave, G. Equilibrium Constants from a Modified Redlich−Kwong Equation of State. *Chem. Eng. Sci.* **1972**, *27*, 1197.
(11) Okuno, R.; Johns, R. T.; Sepehrnoori, K. Three-Phase Flash in Compositional Simulation Using a Reduced Method. *SPE J.* **2010**, *15*, 689.
(12) Memon, A. I.; Gao, J.; Taylor, S. D.; Davies, T. L.; Jia, N. A Systematic Workflow Process for Heavy Oil Characterization. *J. Petrol. Technol.* **2010**, *63*, 89.
(13) Zabel, F.; Law, D.H.-S.; Taylor, S.; Zuo, J. Impact of Uncertainty of Heavy Oil Fluid Property Measurements. *J. Can. Pet. Technol.* **2010**, *49*, 28.
(14) Whitson, C. H.; Brulè, M. R. *Phase Behaviour*, SPE Henry L. Doherty Series, Vol. *20*; SPE: Richardson, TX, 2000.
(15) Pedersen, K. S.; Christensen, P. L. *Phase Behavior of Petroleum Reservoir Fluids*; CRC Press, Taylor & Francis Group: Boca Raton, FL, 2007.
(16) Whitson, C. H. Characterizing Hydrocarbon Plus Fractions. *SPE J.* **1983**, *23*, 683.
(17) Quiñones-Cisneros, S. E.; Zéberg-Mikkelsen, C. K.; Stenby, E. H. Friction Theory Prediction of Crude Oil Viscosity at Reservoir Conditions Based on Dead Oil Properties. *Fluid Phase Equilib.* **2003**, *212*, 233.
(18) Pedersen, K. S.; Thomassen, P.; Fredenslund, Aa. SRK-EOS Calculation for Crude Oils. *Fluid Phase Equilib.* **1983**, *14*, 209.
(19) Pedersen, K. S.; Thomassen, P.; Fredenslund, Aa. Thermodynamics of Petroleum Mixtures Containing Heavy Hydrocarbons. 1. Phase Envelope Calculations by Use of the Soave−Redlich−Kwong Equation of State. *Ind. Eng. Chem. Process Des. Dev.* **1984**, *23*, 163.
(20) Ghasemi, M.; Alavian, S. A.; Whitson, C. H. C_7+ Characterization of Heavy Oil Based on Crude Assay Data. *SPE Heavy Oil Conference and Exhibition*, Kuwait City, Kuwait, Dec. 12−24, 2011; Paper SPE 148906-MS.
(21) Ambrose, D.; Tsonopoulos, C. Vapor−Liquid Critical Properties of Elements and Compounds. 2. Normal Alkanes. *J. Chem. Eng. Data* **1995**, *40*, 531.
(22) Cavett, R. H. Physical Data for Distillation Calculations, Vapor−Liquid Equilibria. *Proc. 27th API Meeting* **1962**, *42*, 351.
(23) Edmister, W. C. Applied Hydrocarbon Thermodynamics, Part 4: Compressibility Factors and Equations of State. *Pet. Refiner.* **1958**, *37*, 173.
(24) Kesler, M. G.; Lee, B. I. Improve Prediction of Enthalpy of Fractions, Hydrocarbon Processing. *Hydrocarbon Process* **1976**, *55*, 153.
(25) Riazi, M. R.; Al-Sahhaf, T. A. Physical Properties of Heavy Petroleum Fractions and Crude Oils. *Fluid Phase Equilib.* **1996**, *117*, 217.
(26) Korsten, H. Internally Consistent Prediction of Vapor Pressure and Related Properties. *Ind. Eng. Chem. Res.* **2000**, *39*, 813.
(27) Riazi, M. R.; Daubert, T. E. Simplify Property Predictions. *Hydrocarbon Process* **1980**, *59*, 115.
(28) Riazi, M. R.; Daubert, T. E. Characterization Parameters for Petroleum Fractions. *Ind. Eng. Chem. Res.* **1987**, *26*, 755.
(29) Twu, C. H. An Internally Consistent Correlation for Predicting the Critical Properties and Molecular Weights of Petroleum and Coal-Tar Liquids. *Fluid Phase Equilib.* **1984**, *16*, 137.
(30) Lee, B. I.; Kesler, M. G. A Generalized Thermodynamic Correlation Based on Three- Parameter Corresponding States. *AIChE J.* **1975**, *21*, 510.
(31) Pedersen, K. S.; Thomassen, P.; Fredenslund, A. Characterization of Gas Condensate Mixtures. *Advances in Thermodynamics*; Taylor & Francis: New York, 1989.
(32) Pedersen, K. S.; Blilie, A. L.; Meisingset, K. K. PVT Calculations on Petroleum Reservoir Fluids Using Measured and Estimated Compositional Data for the Plus Fraction. *Ind. Eng. Chem. Res.* **1992**, *31*, 1378.
(33) Pedersen, K. S.; Milter, J.; Sørensen, H. Cubic Equations of State Applied to HT/HP and Highly Aromatic Fluids. *SPE J.* **2004**, *9*, 186.
(34) Peneloux, A.; Rauzy, E.; Fréze, R. A Consistent Correlation for Redlich−Kwong−Soave Volumes. *Fluid Phase Equilib.* **1982**, *8*, 7.
(35) Jhaveri, B. S.; Youngren, G. K. Three Parameter Modification of the Peng−Robinson Equation of State to Improve Volumetric Predictions. *SPE J.* **1988**, *3*, 1033.
(36) Krejbjerg, K.; Pedersen, K. S. Controlling VLLE Equilibrium with a Cubic EoS in Heavy Oil Modeling. *57th Annual Technical Meeting of the Petroleum Society (Canadian International Petroleum Conference)*, Calgary, Canada, June 13−15, 2006.
(37) Polishuk, I.; Wisniak, J.; Segura, H. Estimation of Liquid−Liquid−Vapor Equilibria in Binary Mixtures of *n*-Alkanes. *Ind. Eng. Chem. Res.* **2004**, *43*, 5957.
(38) Joergensen, M.; Stenby, E. H. Optimization of Pseudocomponents Selection for Compositional Studies of Reservoir Fluids. *Annual Technical Conference and Exhibition*, Dallas, Texas, Oct. 22−25, 1995; Paper SPE 30789.
(39) Wang, P.; Pope, G. A. Proper Use of Equations of State for Compositional Reservoir Simulation. *J. Pet. Technol.* **2001**, *53*, 74.
(40) Lolley, C. S.; Richardson, W. C. Compositional Input for Thermal Simulation of Heavy Oils with Application to the San Ardo Field. *International Thermal Operation & Heavy Oil Symposium*, Bakersfield, California, Dec. 10−12, 1997; Paper SPE 37538.
(41) *PVTsim 20.0*. Calsep A/S: Lyngby, Denmark, 2011.
(42) Christensen, P. L. Regression to Experimental PVT Data. *J. Can. Petro. Technol.* **1999**, *38*, 1.
(43) Voulgaris, M.; Stamatakis, S.; Magoulas, K.; Tassios, D. Prediction of Physical Properties for Nonpolar Compounds, Petroleum, and Coal Liquid Fractions. *Fluid Phase Equilib.* **1991**, *64*, 73.
(44) Lohrenz, J.; Bray, B. G.; Clark, C. R. Calculating Viscosities of Reservoir Fluids from Their Compositions. *J. Pet. Techol.* **1964**, *16*, 1171.
(45) Pitzer, K. S. The Volumetric and Thermodynamic Properties of Fluids. I. Theoretical Basis and Viral Coefficients. *J. Am. Chem. Soc.* **1995**, *77*, 3427.
(46) Pitzer, K. S.; Lippmann, D. Z.; Curl, R. F., Jr.; Huggins, C. M.; Petersen, D. E. The Volumetric and Thermodynamic Properties of Fluids. II. Compressibility Factor, Vapor Pressure, and Entropy of Vaporization. *J. Am. Chem. Soc.* **1955**, *77*, 3433.
(47) Kumar, A.; Okuno, R. Fluid Characterization Using an EOS for Compositional Simulation of Enhanced Heavy-Oil Recovery. *SPE Annual Technical Conference and Exhibition*, San Antonio, TX, Oct. 8−10, 2012; Paper SPE 159494-MS.
(48) Ting, P. D.; Joyce, P. C.; Jog, P. K.; Chapman, W. G.; Thies, M. C. Phase Equilibrium Modeling of Mixtures of Long Chain and Short Chain Alkanes Using Peng−Robinson and SAFT. *Fluid Phase Equilib.* **2003**, *206*, 267.

(49) Voutsas, E. C.; Pappa, G. D.; Magoulas, K.; Tassios, D. P. Vapor Liquid Equilibrium Modeling of Alkane Systems with Equation of State: "Simplicity versus Complexity". *Fluid Phase Equilib.* **2006**, *240*, 127.
(50) Yakoumis, I.; Kontogeorgis, G. M.; Voutsas, E.; Tassios, D. P. Vapor−Liquid Equilibria for Alcohol/Hydrocarbon Systems Using the CPA Equation of State. *Fluid Phase Equilib.* **1997**, *130*, 31.
(51) Kumar, A.; Okuno, R. Critical Parameters Optimized for Accurate Phase Behavior Modeling for Heavy *n*-Alkanes up to C_{100} using the Peng−Robinson Equation of State. *Fluid Phase Equilib.* **2012**, *335*, 46.
(52) Quiñones-Cisneros, S. E.; Zéberg-Mikkelsen, C. K.; Baylaucq, A.; Boned, C. Viscosity Modeling and Prediction of Reservoir Fluids: From Natural Gas to Heavy Oils. *Int. J. Thermophys.* **2004**, *25*, 1353.
(53) Quiñones-Cisneros, S. E.; Dalberg, A.; Stenby, E. H. PVT Characterization and Viscosity Modeling and Prediction of Crude Oils. *Pet. Sci. Technol.* **2004**, *22*, 1309.
(54) Quiñones-Cisneros, S. E.; Andersen, S. I.; Creek, J. Density and Viscosity Modeling and Characterization of Heavy Oils. *Energy Fuels* **2005**, *19*, 1314.
(55) Pan, H.; Firoozabadi, A.; Fotland, E. Pressure and Composition Effect on Wax Precipitation: Experimental Data and Model Results. *SPE Prod. Facil.* **1997**, *12*, 250.
(56) Søreide, I. Improved Phase Behavior Predictions of Petroleum Reservoir Fluids from a Cubic Equation of State, Ph.D. dissertation, Norwegian University of Science and Technology, Trondheim, Norway, 1989.
(57) Kokal, S. L.; Sayegh, S. G. Phase Behavior and Physical Properties of CO_2-Saturated Heavy Oil and its Constitutive Fractions: Experimental Data and Correlations. *J. Pet. Sci. Eng.* **1993**, *9*, 289.
(58) Yazdani, A.; Maini, B. B. Measurements and Modelling of Phase Behavior and Viscosity of a Heavy Oil/Butane System. *J. Can. Pet. Technol.* **2010**, *49*, 9.
(59) Merrill, R. C.; Newley, T. M. J. A Systematic Investigation into the Most Suitable Data for the Development of Equations of State for Petroleum Reservoir Fluids. *Fluid Phase Equilib.* **1993**, *82*, 101.
(60) Egwuenu, A. M.; Johns, R. T.; Li, Y. Improved Fluid Characterization for Miscible Gas Floods. *SPE Reservoir Eval. Eng.* **2008**, *11*, 655.
(61) Pedersen, K. S.; Thomassen, P.; Fredenslund, Aa. Thermodynamics of Petroleum Mixtures Containing Heavy Hydrocarbons. 3. Efficient Flash Calculation Procedures Using the SRK Equation of State. *Ind. Eng. Proc. Des. Dev.* **1985**, *24*, 948.
(62) Zuo, J. Y.; Zhang, D. Plus Fraction Characterization and PVT Data Regression for Reservoir Fluids near Critical Conditions. *SPE Asia Pacific Oil and Gas Conference and Exhibition*, Brisbane, Australia, Oct. 16−18, 2000; Paper SPE 64520-MS.
(63) Mushrif, S. H. Determining Equation of State Binary Interaction Parameters Using K- and L-Points. Master Thesis, The University of Saskatchewan, Saskatoon, Canada, 2004.
(64) Yang, Q. Automatic Development of Global Phase Diagrams for Binary Systems in Pressure-Temperature Space. Master Thesis, the University of Saskatchewan, Saskatoon, Canada, 2004.
(65) Mushrif, S. H.; Phoenix, A. V. Effect of Peng−Robinson Binary Interaction Parameters on the Predicted Multiphase Behavior of Selected Binary Systems. *Ind. Eng. Chem. Res.* **2008**, *47*, 6280.
(66) Gauter, K. Fluid Multiphase Behavior in Ternary Systems of Near-Critical CO_2. PhD dissertation, The Technical University of Berlin, Berlin, Germany, 1999.
(67) Gauter, K.; Heidemann, R. A.; Peters, C. J. Modeling of Fluid Multiphase Equilibria in Ternary Systems of Carbon Dioxide as the Near-Critical Solvent and Two Low-Volatile Solutes. *Fluid Phase Equilib.* **1999**, *158−160*, 133.
(68) Satyro, M. A.; Shaw, J. M.; Yarranton, H. W. A Practical Method for the Estimation of the Oil and Water Mutual Solubilities. *Fluid Phase Equilib.* **2013**, *355*, 12.
(69) Pedersen, K. S.; Thomassen, P.; Fredenslund, A. On the Dangers of Tuning Equation of State Parameters. *Chem. Eng. Sci.* **1988**, *43*, 269.
(70) Michelsen, M. L. Simplified Flash Calculation for Cubic Equation of State. *Ind. Eng. Chem. Process Des. Dev.* **1986**, *25*, 184.
(71) Heidemann, R. A.; Michelsen, M. L. Instability of Successive Substitution. *Ind. Eng. Chem. Res.* **1995**, *34*, 958.
(72) Okuno, R.; Johns, R. T.; Sepehrnoori, K. Mechanisms for High Displacement Efficiency of Low-Temperature CO_2 Floods. *SPE J.* **2011**, *16*, 751.
(73) Johns, R. T.; Orr, F. M., Jr. Miscible Gas Displacement of Multicomponent Oils. *SPE J.* **1996**, *1*, 39.
(74) Ahmadi, K.; Johns, R. T. Multiple Mixing-Cell Model for MMP Determination. *SPE J.* **2011**, *16*, 733.
(75) PennPVT Toolkit, Gas Flooding Joint Industrial Project, Director: Dr. Russell T. Johns, EMS Energy Institute, The Pennsylvania State University, University Park, PA.
(76) *CMG User Manual 2011*; Computer Modeling Group, Calgary, Canada, 2011.
(77) Coats, K. H.; Smart, G. T. Application of a Regression Based EOS PVT Program to Laboratory Data. *SPE Res. Eng.* **1986**, *1*, 277.
(78) Cullick, A. S.; Pebdani, F. N.; Griewank, A. K. Modified Corresponding States Method for Predicting Densities of Petroleum Reservoir Fluids. *Ind. Eng. Chem. Res.* **1989**, *28*, 340.